

See discussions, stats, and author profiles for this publication at: <https://www.researchgate.net/publication/258656262>

Analysis of Temperature Effect on p-i-n Diode Circuits by a Multiphysics and Circuit Cosimulation Algorithm

Article in IEEE Transactions on Electron Devices · November 2012

DOI: 10.1109/TED.2012.2211602

CITATIONS

23

READS

85

5 authors, including:



Changjun Liu

Sichuan University

196 PUBLICATIONS 2,500 CITATIONS

[SEE PROFILE](#)



Kama Huang

Sichuan University

315 PUBLICATIONS 4,354 CITATIONS

[SEE PROFILE](#)



Xiao Bang

Beijing Normal University

48 PUBLICATIONS 708 CITATIONS

[SEE PROFILE](#)

Analysis of Temperature Effect on p-i-n Diode Circuits by a Multiphysics and Circuit Cosimulation Algorithm

Jun-quan Chen, Xing Chen, *Senior Member, IEEE*, Chang-Jun Liu, *Senior Member, IEEE*, Kama Huang, *Senior Member, IEEE*, and Xiao-Bang Xu, *Senior Member, IEEE*

Abstract—A novel cosimulation algorithm that combines physical-model-based multiphysics simulation with equivalent-model-based circuit simulation is proposed. In the algorithm, multiphysics simulation couples multiple physical equations (e.g., the electromagnetic, semiconductor transport, thermodynamics equations, etc.) to be solved numerically by an iterative approach. The multiphysics simulation is for modeling the electrothermal behavior of semiconductor devices, and then, it is incorporated into the circuit simulation to extend the simulation from semiconductor devices to circuits. Employing the proposed algorithm, sample numerical results for the temperature effect on circuits comprising commercial p-type–intrinsic–n-type diodes with a model number of `mot_bal991t1` are obtained and compared to measurement data. The comparison shows a good agreement between these two sets of data, which validates the feasibility and accuracy of the proposed algorithm. Moreover, the proposed algorithm can provide a useful physical mechanism for understanding temperature effect on semiconductor devices and circuits.

Index Terms—Circuit simulation, multiphysics, semiconductor, temperature effect.

I. INTRODUCTION

TEMPERATURE has a significant impact on the performance of semiconductor devices and circuits because variation in temperature may change the mobility of electrons and holes, as well as the material properties in the devices. Hence, temperature analysis of semiconductor devices and circuits has been a subject of increasing interest for many years [1]–[3]. In the literature, a number of electrothermal analyses for semiconductor devices and circuits have been reported, employing various methods to describe the temperature characteristics of semiconductor devices [1]–[10]. For example, finite-difference and finite-element simulation [4], [5], analytical methods [6],

[7], and thermal resistance and thermal capacitance network element analysis [8], [9] are utilized for solving the heat diffusion equation, and some thermal models are derived and extracted from experimental results [10]. In addition, the thermal models are coupled to the compact equivalent-circuit electrical models based on knowledge of the power dissipated in the semiconductor devices to formulate electrothermal model analysis [2], [3]. However, those approaches suffer from limitations that may preclude their application in some cases. The thermal resistance and thermal capacitance network element analysis is fundamentally an approximation and thus are inadequate for modeling some kinds of semiconductor devices, such as power devices [11]. The extracted thermal models vary for different semiconductor devices under various conditions. Therefore, deriving the thermal models is a heavy experimental burden, and it is impossible to cover all the different cases. The equivalent-circuit electrical models may lose their accuracy in some special cases such as high-power or high-frequency applications. Moreover, most of them lack direct physical interpretation [12] and thus cannot be easily used to predict the physical effect of the semiconductor devices and circuits.

An existing method for the electrothermal analysis of semiconductor devices is the physical-model-based multiphysics simulation [13], [14]. This method is essentially a coupled-field analysis, which allows users to study the combined effects of multiple physical phenomena (fields). In the analysis, multiple physical equations (e.g., the electromagnetic, semiconductor transport, and thermodynamic equations) are coupled to form a system of equations, and then, the system of equations is solved numerically.

However, the physical-model-based multiphysics simulation is very complicated and costs much computation time, even for a single semiconductor device. Hence, for a circuit that contains various electronic devices and whose dimensions are much larger than those of a single semiconductor device, it is difficult to be analyzed employing a multiphysics simulation. Researchers have devoted significant effort to develop a thermal model reduction technique [11], [15], [16] that represents the thermal characteristics of a circuit by utilizing the so-called thermal nodes and thus performs the coupled electrothermal simulation at the circuit level. However, this technique requires explicit lumped-element RC network approximation or nodal reduction, and it usually assumes the thermal subsystem to be linear.

Manuscript received November 17, 2011; accepted July 24, 2012. Date of publication August 27, 2012; date of current version October 18, 2012. The work of J.-Q. Chen, X. Chen, C.-J. Liu, and K. Huang was supported in part by the China National Nature Science Foundation-China Academy of Engineering Physics Foundation Fund under Grant 10876020 and by the New Century Excellent Talent Program in China under Grant NCET-08-0369. The review of this paper was arranged by Editor R. Venkatasubramanian.

J.-Q. Chen, X. Chen, C.-J. Liu, and K. Huang are with the College of Electronic and Information Engineering, Sichuan University, Chengdu 610064, China (e-mail: xingcsc@yahoo.com.cn).

X.-B. Xu is with the Holcombe Department of Electrical and Computer Engineering, Clemson University, Clemson, SC 29634-0915 USA.

Digital Object Identifier 10.1109/TED.2012.2211602

In the authors' previous work [17], a cosimulation algorithm is proposed, which incorporates the physical-model-based field simulation into an equivalent-model-based circuit simulation to simulate the electrical characteristics of circuits. This work extends the cosimulation algorithm to analyze temperature effect on circuits. In the algorithm, the multiphysics simulation is employed for analyzing the crucial and sensitive semiconductor devices in a circuit, and then, a cosimulation algorithm that incorporates the multiphysics simulation into an equivalent-model-based circuit simulation is utilized to estimate the electrothermal behavior of a whole circuit. Since the multiphysics simulation is based on a physical model, it is naturally able to accurately simulate the electrothermal behavior of semiconductor devices under various conditions, and it can be used for predicting the physical effect; on the other hand, the equivalent-model-based simulation at the circuit level can avoid employing the multiphysics simulation to analyze a whole circuit and thus greatly reduce the computation burden.

In this paper, the proposed cosimulation algorithm is applied to analyze temperature effect on circuits comprising commercial p-i-n diodes with model number mot_bal99lt. Then, a serial of experiments are conducted to validate the proposed algorithm. The remainder of this paper is organized as the follows: The proposed cosimulation algorithm is formulated in Section II. Then, in Section III, the simulation results of temperature effect on p-i-n diode circuits are presented and compared to measurement data. Finally, conclusions are drawn in Section IV.

II. PRINCIPLE AND FORMULATION OF THE COSIMULATION ALGORITHM

A. Multiphysics Simulation for Semiconductor Devices

In principle, the electrothermal behavior of semiconductor devices can be described by a multiphysics equation system coupling the following physical equations [14]:

1) Poisson Equation:

$$\nabla^2 \varphi = -\frac{q}{\varepsilon}(p - n + N_t) \quad (1)$$

where φ is the electrostatic potential; ε is the permittivity; q is the elementary charge; n and p are the electron and hole concentration, respectively; and N_t is the doping concentration.

This equation, which describes electromagnetic field variation inside semiconductor devices, is reduced from the Maxwell equations based on the fact that the active region of semiconductor devices is much smaller than the minimum wavelength of signals. For most semiconductor devices, this approximation holds for frequencies up to gigahertz [18], even terahertz [19], [20].

2) Continuity Equations for Electrons and Holes:

$$\frac{\partial n}{\partial t} = \frac{1}{q} \nabla \cdot \vec{J}_n - R \quad (2)$$

$$\frac{\partial p}{\partial t} = -\frac{1}{q} \nabla \cdot \vec{J}_p - R \quad (3)$$

where t is the time; \vec{J}_n and \vec{J}_p denote the current densities caused by electrons and holes, respectively; and R is the electron-hole recombination rate.

3) Current Equations With Temperature Effect [21]:

$$\vec{J}_n = \mu_n k_b (T \nabla n + n \nabla T) + q \mu_n n \nabla \varphi \quad (4)$$

$$\vec{J}_p = -\mu_p k_b (T \nabla p + p \nabla T) + q \mu_p p \nabla \varphi \quad (5)$$

$$\begin{aligned} I &= A(\vec{J}_c + \vec{J}_d) \cdot \vec{\delta} \\ &= A \left(\vec{J}_n + \vec{J}_p + \varepsilon \frac{\partial \vec{E}}{\partial t} \right) \cdot \vec{\delta} \end{aligned} \quad (6)$$

where μ_n and μ_p are the effective mobility of electrons and holes; T is the temperature; k_b is the Boltzmann constant; I is the branch current; \vec{J}_c and \vec{J}_d are the conduction current density and the displacement current density, respectively; A is the cross-sectional area; and $\vec{\delta}$ is a unit vector normal to the cross section.

The continuity equations (2) and (3), together with the current equations (4)–(6), are the drift-diffusion approximation for the Boltzmann transport theory [22], which reveals the physics of carrier transport inside semiconductor devices for the sake of simplicity.

4) Heat Diffusion Equations:

$$\rho c \frac{\partial T}{\partial t} = \nabla \cdot [\kappa(T) \nabla T] + g \quad (7)$$

$$g = \left(\vec{J}_n + \vec{J}_p + \varepsilon \frac{\partial \vec{E}}{\partial t} \right) \cdot \vec{E} \quad (8)$$

where $\kappa(T)$ is the temperature-dependent thermal conductivity, ρ is the specific mass density, c is the specific heat capacity, and g is the rate of heat generation.

5) Characteristic Parameter Equations:

$$\varepsilon(T) = \varepsilon [1 + B_\varepsilon (T - 300)] \quad (9)$$

$$N_i(T) = N_s \exp \left(-\frac{E_g}{2k_b T} \right) \quad (10)$$

$$\mu_{n,p}(T) = \mu_{n,p}^0 \times \frac{(T/T_0)^{-\alpha}}{(1 + (E/E_c)^\beta)^{\frac{1}{\beta}}} \quad (11)$$

$$\tau_{n,p}(T) = \tau_{n,p}^0 \times \left(\frac{T}{T_0} \right)^\gamma \quad (12)$$

where B_ε is the Blakemore constant; N_i is the intrinsic carrier concentration, i.e., the number of electrons in the conduction band (and also the number of holes in the valence band) per unit volume in semiconductor that is completely free of impurities and defects; N_s is the effective density of states in the conduction band; E_g is the energy gap; $\mu_{n,p}^0$ are the effective mobility of electrons and holes at room temperature $T_0 = 300$; $\tau_{n,p}^0$ are the lifetime of electrons and holes at room temperature $T_0 = 300$; E_c is the critical field; and α , β , and γ are coefficients.

These equations relate the temperature with some characteristic parameters [22], such as the permittivity (9), the intrinsic carrier concentration (10), the effective mobility of electrons and holes (11), and the lifetime of electrons and holes (12).

Equations (1)–(12) form a multiphysics equation system, which is a system of coupled nonlinear partial differential equations. Practically, it is impossible to obtain closed-form solutions of such a set of equations. Hence, an iterative numerical method is employed to solve this system of equations. Let us refer, for the sake of simplicity, to a 1-D physical model that is taken in consideration in the present implementation of this work.

The electrical part of the system (1)–(6), as T is a known value, can be solved using the method described in [23]. The whole procedure can be simplified to the solution of an increment equation

$$\mathbf{A}\Delta\mathbf{y}_{(k-1)} + \mathbf{B}\Delta\mathbf{y}_{(k)} + \mathbf{C}\Delta\mathbf{y}_{(k+1)} = \mathbf{H}_{(k)} \quad (13)$$

where $y = [\varphi \ n \ p]^T$; $\Delta y = [\Delta\varphi \ \Delta n \ \Delta p]^T$; \mathbf{A} , \mathbf{B} , and \mathbf{C} are 3×3 matrices; and \mathbf{H} is a 3×1 matrix.

Based on the thermal equilibrium and zero space-charge condition, for a semiconductor device located between $x = 0$ and $x = w$, it can be described as

$$n_0 p_0 = n_w p_w = 0 \quad (14a)$$

$$N_{t0} + p_0 - n_0 = N_{tw} + p_w - n_w = 0 \quad (14b)$$

$$\varphi_0 = U_j \left(\frac{k_b T}{q} \right) \ln \left(\frac{p_0}{N_i} \right) \quad (14c)$$

$$\varphi_w = \left(\frac{k_b T}{q} \right) \ln \left(\frac{n_w}{N_i} \right) \quad (14d)$$

where U_j is a given terminal voltage. Then, the increment equation (13) can be solved by using the chasing method [24].

For the thermal equation (7), as n , p , and φ are known values and in view of the principle described in [25] that the partial differential equation may be discretized into a finite number of first-order ordinary time-dependent differential equations, it can be rewritten as

$$\frac{T_{k+1} - T_k}{h_{k,k+1}} - \frac{T_k - T_{k-1}}{h_{k-1,k}} + g = \frac{dC_k \cdot T_k}{dt} \quad (15)$$

where C_k and $h_{k,k+1}$ are the discretization coefficients. By using the Newton iteration method, the increment equation can be rewritten as

$$a\Delta y_{(k-1)} + b\Delta y_{(k)} + c\Delta y_{(k+1)} = h \quad (16)$$

where $y = [T]$; $\Delta y = [\Delta T]$; and a , b , c , and h are the coefficients. Based on the thermal boundary condition [1], i.e., the convection boundary condition

$$\frac{\partial T}{\partial r} = -h_c(T - T_a) \quad (17)$$

where T_a and h_c represent the ambient temperature and convection coefficient, respectively, the increment equation (16) can also be solved by using the chasing method.

The iterative procedure for the multiphysics simulation is given here.

- 1) Initializing the parameters such as terminal voltages U_j and ambient temperature T_0 .
- 2) Solving the increment equation (13) to get the electrical characteristics of the semiconductor device and updating the corresponding parameters n , p , and φ .
- 3) Using the updated parameters n , p , and φ to solve the increment equation (16) to get the thermal characteristics of the semiconductor device and then obtaining the variation of the temperature ΔT_0 .
- 4) Updating the characteristic parameters ε , N_i , μ_n , and μ_p by employing the previously obtained parameters n , p , φ , and T_0 . In this way, the electrical and thermal effect on the semiconductor device are considered simultaneously and correlated to each other in the simulation.
- 5) Repeating steps 2–4 using the updated temperature $T_0 + \Delta T_0$ until reaching a convergence criterion, which may be defined as the temperature variation ΔT_0 being less than a preset smaller value.
- 6) The final temperature T_0 and the electrical parameters n , p , and φ are used to obtain the branch current I_j in the device from (6).

In this way, the corresponding branch current I_j in a semiconductor device can be simulated for the given terminal voltage U_j under the temperature effect. In other words, in the macroscopic view, the electrothermal behavior of the semiconductor device is represented by the relationship between the terminal voltage U_j and the branch current I_j in the multiphysics simulation.

B. Multiphysics and Circuit Cosimulation Algorithm

For a circuit, using the modified nodal analysis method described in [26], its simulation can be simplified to the solution of a system of equations

$$\begin{cases} f_1(U_1, U_2, \dots, U_k) = 0 \\ f_2(U_1, U_2, \dots, U_k) = 0 \\ \vdots \\ f_k(U_1, U_2, \dots, U_k) = 0 \end{cases} \quad (18)$$

where U is the node voltage, and k is the index of the node. Using the Newton–Raphson algorithm, the solution procedure of the nonlinear (18) is converted to an iterative operation, with the iterative equations [26]

$$\mathbf{U}^{n+1} = \mathbf{U}^n - \mathbf{J}^{-1}(\mathbf{U}^n)\mathbf{f}(\mathbf{U}^n) \quad (19)$$

where $\mathbf{U} = [U_1, U_2, \dots, U_k]^T$, $\mathbf{f}(\mathbf{U}) = [f_1(\mathbf{U}), f_2(\mathbf{U}), \dots, f_k(\mathbf{U})]^T$, n is the iteration index, and \mathbf{J} is the Jacobian matrix

$$\mathbf{J} = \begin{bmatrix} \frac{\partial f_1}{\partial U_1} & \cdots & \frac{\partial f_1}{\partial U_k} \\ \vdots & \ddots & \vdots \\ \frac{\partial f_k}{\partial U_1} & \cdots & \frac{\partial f_k}{\partial U_k} \end{bmatrix}. \quad (20)$$

For a device in the circuit, its branch currents are related to the terminal voltages. For example, assuming a device is located

in the j th branch and between the $(k-1)$ th and k th nodes, the relationship between the branch current I_j and the given terminal voltages U_{k-1} and U_k can be described as

$$I_j = \psi(U_k, U_{k-1}). \quad (21)$$

To simplify the simulation and reduce the computation burden, in this work, only the crucial and sensitive semiconductor devices in the circuit are simulated by the previously introduced multiphysics simulation. As for other circuit elements, such as resistors, capacitors, etc., (21) can be derived from their equivalent-circuit models that can be established from the devices' manuals or some circuit simulation softwares.

Substituting (21) into (20) and using two trial solutions U_{k-1}^Δ and U_k^Δ to approximately calculate the partial derivatives of I_j , we can express a matrix element in (20) by

$$\begin{aligned} \frac{\partial f_j}{\partial U_k} &= \frac{\partial f_j}{\partial I_j} \frac{\partial I_j}{\partial U_k} + \frac{\partial f_j}{\partial U_k} = \frac{\partial \psi(U_{k-1}, U_k)}{\partial U_k} + \frac{\partial f_j}{\partial U_k} \\ &\approx \frac{\psi(U_{k-1}, U_k^\Delta) - \psi(U_{k-1}, U_k)}{U_k^\Delta - U_k} + \frac{\partial f_j}{\partial U_k}. \end{aligned} \quad (22)$$

Then, the iterative equation (19) are rewritten as

$$\begin{aligned} \mathbf{U}^{n+1} &= \mathbf{U}^n \\ - \begin{bmatrix} \frac{\partial f_1^n}{\partial U_1^n} & \cdots & \frac{\partial f_1^n}{\partial I_j^n} \Delta_1 + \frac{\partial f_1^n}{\partial U_{k-1}^n} & \frac{\partial f_1^n}{\partial I_j^n} \Delta_2 + \frac{\partial f_1^n}{\partial U_k^n} \\ \frac{\partial f_2^n}{\partial U_1^n} & \cdots & \frac{\partial f_2^n}{\partial I_j^n} \Delta_1 + \frac{\partial f_2^n}{\partial U_{k-1}^n} & \frac{\partial f_2^n}{\partial I_j^n} \Delta_2 + \frac{\partial f_2^n}{\partial U_k^n} \\ \vdots & \ddots & \vdots & \vdots \\ \frac{\partial f_k^n}{\partial U_1^n} & \cdots & \frac{\partial f_k^n}{\partial I_j^n} \Delta_1 + \frac{\partial f_k^n}{\partial U_{k-1}^n} & \frac{\partial f_k^n}{\partial I_j^n} \Delta_2 + \frac{\partial f_k^n}{\partial U_k^n} \end{bmatrix}^{-1} \mathbf{f}(\mathbf{U}^n) \end{aligned} \quad (23)$$

in which

$$\Delta_1 = \frac{\psi(U_{k-1}^\Delta, U_k^n) - \psi(U_{k-1}^n, U_k^n)}{U_{k-1}^\Delta - U_{k-1}^n}$$

$$\Delta_2 = \frac{\psi(U_{k-1}^n, U_k^\Delta) - \psi(U_{k-1}^n, U_k^n)}{U_k^\Delta - U_k^n}$$

$$U_{k-1}^\Delta = U_{k-1}^n + \Delta$$

$$U_k^\Delta = U_k^n + \Delta$$

where Δ is a small constant (such as 1.0×10^{-6}) selected based on experience for a convergent solution.

To obtain the transient response of a circuit, the simulation procedure is divided into many time intervals. It starts from an initial state of the circuit, which is usually—although not necessarily—the dc state, and proceeds until reaching a time required by the simulation. For each time interval, (23) is solved repeatedly until its convergence condition is satisfied. In the iterative matrix of (23), the terms $\psi(U_{k-1}^n, U_k^n)$, $\psi(U_{k-1}^\Delta, U_k^n)$, and $\psi(U_{k-1}^n, U_k^\Delta)$ for crucial semiconductor devices are obtained by the multiphysics simulation, whereas that for other devices are derived from the circuit simulation based on the equivalent-circuit models [26]. In this way, the multiphysics simulation and the circuit simulation are integrated into a unified algorithm.



Fig. 1. p-i-n diode with model number mot_bal99lt1.

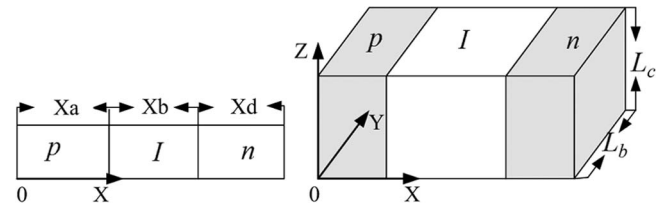


Fig. 2. One-dimensional and 3-D physical model of a p-i-n diode.

III. APPLICATIONS OF THE PROPOSED ALGORITHM

In this section, the proposed cosimulation algorithm is employed for the analysis of temperature effect on circuits comprising commercial p-i-n diodes with model number mot_bal99lt1. The p-i-n diode is depicted in Fig. 1, where its physical dimension is compared to a one-Yuan coin. To validate the proposed algorithm, the simulated results are compared to the experimental data.

A. Physical Model of the mot_bal99lt1 p-i-n Diodes and Its Parameters Extracted by a GA-Based Curve-Fitting Approach

The physical model of a p-i-n diode is shown in Fig. 2. Using the GA-based curve-fitting approach, which has been introduced in the author's previous work [17], and from the measured dc volt-ampere curve, the 1-D physical parameters of the mot_bal99lt1 p-i-n diode are extracted as follows: the lifetime $\tau_p^0 = 5.0 \times 10^{-9} s$ and $\tau_n^0 = 5.0 \times 10^{-9} s$ for p - and n -type carriers, respectively; the thickness of p -layer $X_a = 5.0 \mu m$, i -layer $X_b = 1.55 \mu m$, and n -layer $X_d = 0.5 \mu m$; the cross-sectional area $A = 0.7 \text{ cm}^2$; the coefficient $N_a = 1.8 \times 10^{16} / \text{cm}^3$; $N_b = 0.5 \times 10^{10} / \text{cm}^3$; and $N_d = 1.8 \times 10^{16} / \text{cm}^3$. The doping profile is shown in Fig. 3.

B. Temperature Effect on the DC Characteristics of the mot_bal99lt1 p-i-n Diode

The dc volt-ampere curve of the p-i-n diode at different ambient temperatures T_a ranging from 27°C to 200°C is simulated by the proposed cosimulation algorithm and compared with that obtained from experiment and ADS, which is a famous circuit simulation software based on the equivalent

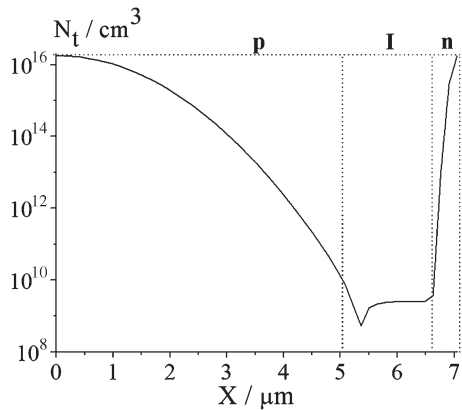


Fig. 3. Doping profile of the p-i-n diode.

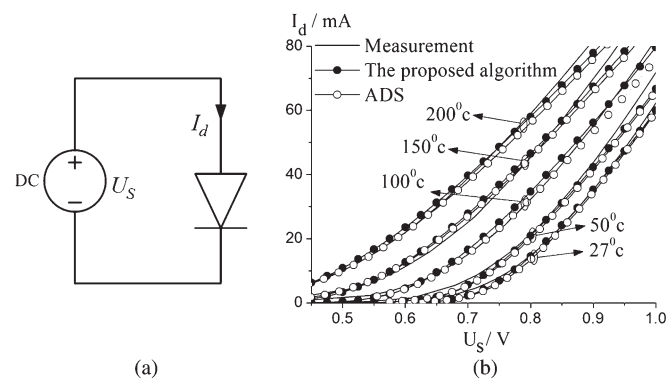


Fig. 4. (a) Test circuit. (b) DC volt-ampere curves at different ambient temperatures.

circuit model, as shown in Fig. 4. From the comparison, one observes that they are in good agreement, which validates the accuracy of the proposed algorithm. In addition, the results illustrate that the branch current of the p-i-n diode becomes larger as the ambient temperature increases.

Fig. 4 also demonstrates that the simulation results generated by the proposed algorithm are closer to the measurement results than those obtained from ADS, particularly when dc voltage U_S becomes high. To further compare the precision of the two simulation methods, the dc voltage is extended to higher than 2.0 V (in such case, branch current I_d may rise up to 500 mA). Fig. 5 depicts the simulation errors, which are defined as the discrepancy between the simulation and measurement results, of the two methods at room ambient temperature $T_a = 27^\circ\text{C}$. It is obvious that the simulation error becomes bigger with the rise of the dc voltage, but the proposed algorithm possesses much higher precision, in comparison with ADS.

When a large branch current goes through a p-i-n diode, it would generate heat due to its ohmic dissipation, which can be calculated by the heat diffusion equation (16) in the proposed algorithm. Fig. 6 presents the measured and simulated temperature T_s on the p-i-n diode's surface at room ambient temperature $T_a = 27^\circ\text{C}$. The simulated and measured results shown in this figure agree with each other and clearly illustrate the heating effect of the large branch current. However, it is worth noting that ADS does not possess the capacity of simulating the heating effect of a large current due to lack

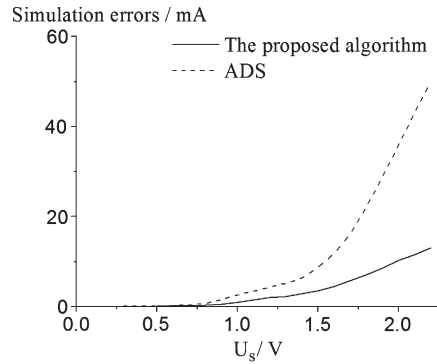


Fig. 5. Simulation errors of the proposed approach and ADS against the dc voltage U_S at room ambient temperature $T_a = 27^\circ\text{C}$.

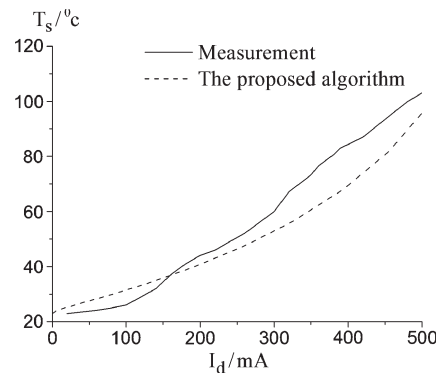


Fig. 6. Measured and simulated temperature on the p-i-n diode's surface at room ambient temperature $T_a = 27^\circ\text{C}$.

of related equivalent models, and this deficiency makes ADS unable to accurately simulate a p-i-n diode with a large branch current, just as what has been illustrated in Fig. 5.

Moreover, the previously inferred temperature effect, i.e., the branch current of the p-i-n diode becomes larger as the ambient temperature increases, can be clearly and intuitively analyzed by the proposed cosimulation algorithm. As depicted in Fig. 7, the simulation results of the proposed algorithm indicate that the p-i-n diode's intrinsic carrier concentration N_i would rise with the ambient temperature. In particular, the intrinsic carrier concentration N_i inside the p-i-n diode is only on the order of $1.0 \times 10^{10}/\text{cm}^3$ at $T_a = 27^\circ\text{C}$, but it would be up to be on the order of $1.0 \times 10^{14}/\text{cm}^3$ at $T_a = 200^\circ\text{C}$. The rise of the intrinsic carrier concentration leads to the increase in carrier concentration but a drop in the effective mobility of carriers inside the p-i-n diode, as illustrated in Figs. 8 and 9. However, the increase in carrier concentration is much higher than the drop of effective mobility, which brings about the increase in conduction current inside the p-i-n diode and finally results in the enhancement of the p-i-n diode's branch current that is composed solely of the conduction current under a dc terminal voltage.

In this example, the proposed cosimulation algorithm demonstrates great advantages in comparison with the equivalent-model-based circuit simulation, e.g., higher simulation precision, capacities of simulating the heating effects caused by a large current and providing the physical mechanism for semiconductor devices and circuits.

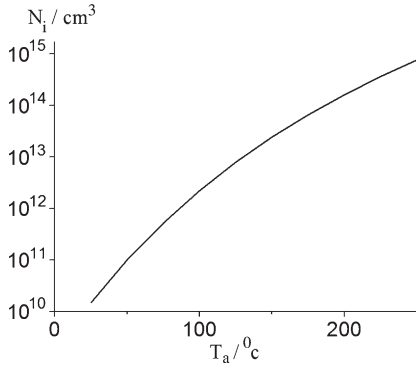


Fig. 7. Intrinsic carrier concentration inside the p-i-n diode versus the ambient temperature.

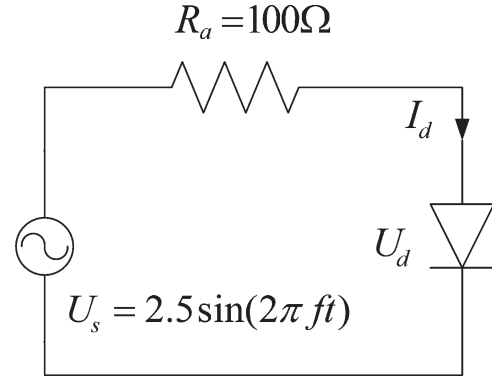


Fig. 10. Circuit containing a mot_bal991t1 p-i-n diode.

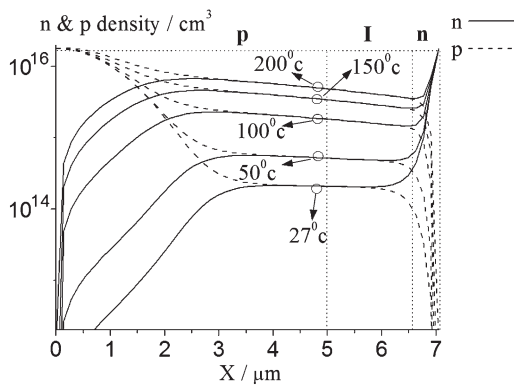


Fig. 8. Carrier concentration of the p-i-n diode at different ambient temperatures ($U_S = 0.5$ V).

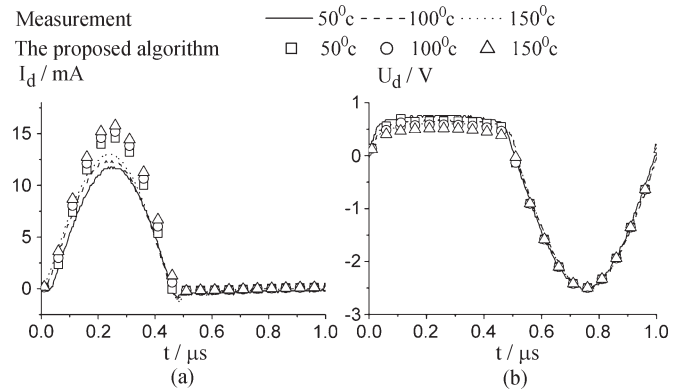


Fig. 11. Measured and simulated branch current and terminal voltage for the p-i-n diode circuit under different ambient temperatures. (a) Branch current. (b) Terminal voltage.

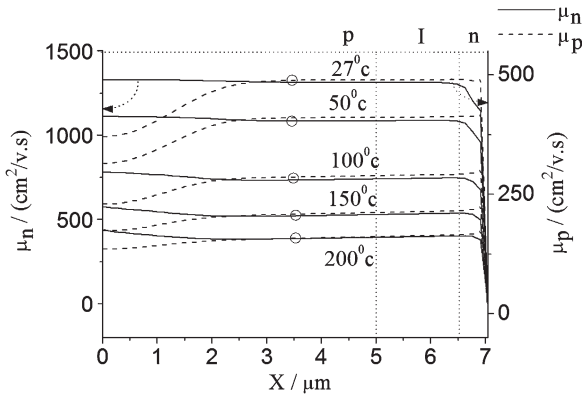


Fig. 9. Effective mobility of electrons and holes of the p-i-n diode at different ambient temperatures ($U_S = 0.5$ V).

C. Temperature Effect on the AC Characteristics of the p-i-n Diode

Fig. 10 shows a circuit consisting of a mot_bal991t1 p-i-n diode, an ac source with voltage $U_s = 2.5$ V, and a resistor $R_a = 100 \Omega$. Its ac characteristics at frequencies of 1 MHz and under different ambient temperatures (50 °C, 100 °C, and 150 °C) are simulated by the proposed algorithm. The simulation results are compared to the measurement data obtained by using a Tektronix TDS1012 oscillograph and a ZTE-202-00AB thermostatic system.

As shown in Fig. 11, the measured and simulated results are in good agreement, despite only a little discrepancy in the peak value of direct current. The branch current goes up with the increase in ambient temperature, and the threshold level of the p-i-n diode slightly decreases with the increase in the ambient temperature in the forward-voltage period.

As just explained in the last section, the rise in ambient temperature leads to the increase in the p-i-n diode’s intrinsic carrier concentration, which brings about a rise in the carrier concentration, as shown in Fig. 12, and a drop in the effective mobility of carriers inside the p-i-n diode, as depicted in Fig. 13. In addition, they, in turn, result in an enhancement of the conduction current. Under an ac terminal voltage, there exist two kinds of current densities inside a p-i-n diode, i.e., the conduction current density \vec{J}_c and the displacement current density \vec{J}_d . The former $\vec{J}_c = \vec{J}_n + \vec{J}_p$ is due to the drift-diffusion movement of the n- and p-type charge carriers, and the latter $\vec{J}_d = \epsilon(\partial\vec{E}/\partial t)$ is caused by variation of the electric field inside the diode. For a p-i-n diode during the forward voltage period, it is in turn-on state, and its displacement current density is negligible in comparison with the conduction current density, as shown in Fig. 14, because the electric field varies slowly at a frequency of 1 MHz. Hence, a rise in the conduction current also results in considerable increase in branch current in the p-i-n diode, with the ambient temperature just like that under a dc terminal voltage. Meanwhile, a higher carrier concentration means that the p-i-n diode has better electrical

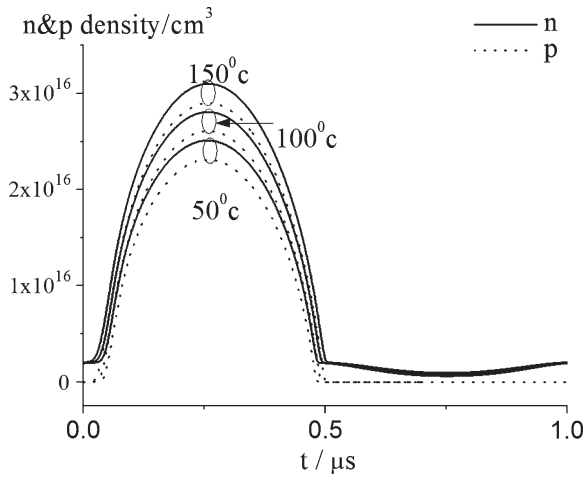


Fig. 12. Carrier concentration inside the center *i*-layer of the p-i-n diode.

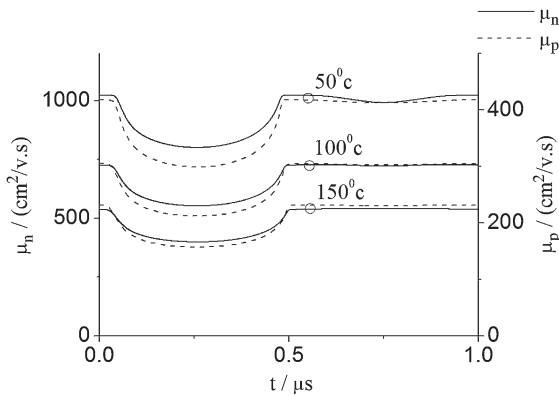


Fig. 13. Effective mobility of carriers inside the center *i*-layer of the p-i-n diode.

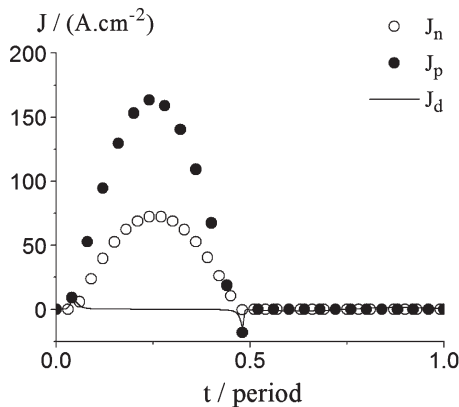


Fig. 14. Simulated current densities at the center of the *i*-layer under ambient temperature $T_a = 50^\circ\text{C}$.

conductivity and can be in turn-on state, even under a lower positive terminal voltage, which results in a slight decrease in the diode’s threshold level.

D. Temperature Effect on a p-i-n Diode Limiter

To further demonstrate the capacity and accuracy of the proposed cosimulation algorithm, it is applied in the analysis of a limiter, as shown in Fig. 15, consisting of two mot_bal99lt1

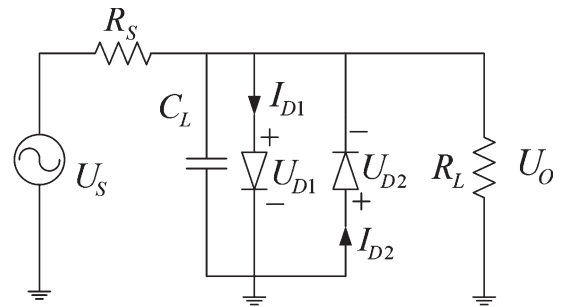


Fig. 15. Limiter circuit composed of two mot_bal99lt1 p-i-n diodes.

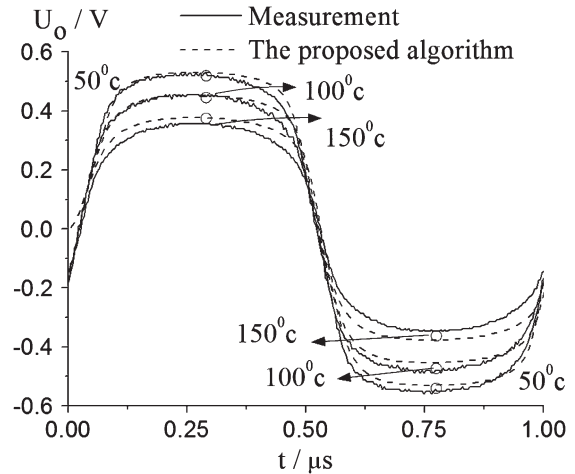


Fig. 16. Measured and simulated waveforms of U_o under different ambient temperatures.

p-i-n diodes, an ac source with voltage $U_s = 2.5\text{ V}$ and the frequency of 1 MHz, two resistors ($R_s = 1\text{ k}\Omega$ and $R_L = 1\text{ k}\Omega$), and a capacitor $C_L = 22\text{ pF}$. The characteristics of the limiter at the frequency of 1 MHz and under different ambient temperatures are simulated by the proposed algorithm and are measured by a Tektronix TDS1012 oscillograph and a ZTE-202-00AB thermostatic system.

Fig. 16 compares the measured and simulated voltage waveforms of the limiter’s output voltage U_o under different ambient temperatures (e.g., 50 °C, 100 °C, and 150 °C). From the comparison, one observes that the two sets of data are in good agreement, which demonstrates the capacity and accuracy of the proposed algorithm for simulating a relatively complicated circuit.

The output voltage U_o ranges from 0.36 to 0.53 V with an exciting voltage $U_s = 2.5\text{ V}$, which clearly illustrates the limiting effect of the limiter. Meanwhile, it can be observed from the figure that the clipping voltage of the limiter slightly decreases with the increase in ambient temperature. For the limiter, two p-i-n diodes are connected in parallel, so that, at any time, one of them is in turn-on state. Because the diode’s threshold level decreases with the increase in the ambient temperature, as pointed out in the last section, the slightly decrease in the threshold level makes the limiter’s clipping voltage decrease with the increase in the ambient temperature.

In this paper, the proposed algorithm was coded in FORTRAN and implemented on a personal computer equipped with an Intel Q6600 processor of four cores and 4-GB memory.

The central processing unit (CPU) time needed for the proposed algorithm mainly depends on the number of meshes for discretizing the physical model of the device. Because this work employs the p-i-n diode's 1-D physical model with 50 meshes, the CPU time for the proposed algorithm is short, about 20 s for the simple circuits presented in Figs. 4 and 10, and about 50 s for the limiter circuit shown in Fig. 15.

IV. CONCLUSION

The temperature effect is very important to electronic devices and circuits. A cosimulation algorithm that combines the multiphysics simulation and the circuit simulation has been proposed in this paper. A physical-model-based multiphysics simulation has been used for the electrothermal analysis of the crucial and sensitive semiconductor devices in a circuit. Then, it has been combined with an equivalent-model-based circuit simulation to get the electrothermal behavior of the whole circuit. This algorithm has the accuracy and versatility of the physical-model-based multiphysical simulation, as well as the simplicity and efficiency of the equivalent-model-based circuit simulation.

Making use of the proposed cosimulation algorithm, sample numerical results of the temperature effect on p-i-n diode circuits are obtained, presented, and analyzed in this work. The numerical results agree with the measurement data well, even for a relatively complicated circuit such as a p-i-n diode limiter, which validates the accuracy and capacity of the proposed algorithm. Furthermore, the proposed algorithm is capable of depicting useful physical mechanisms for the analysis of the temperature effect on semiconductor devices and circuits. Moreover, the proposed algorithm can be extended to more comprehensive and complicated models with no need for significant modifications. In the future, this algorithm will be employed for the analysis of more semiconductor devices such as bipolar junction transistors and field-effect transistors, as well as their circuits.

REFERENCES

- [1] T. Bechtold, E. B. Rudnyi, and J. G. Korvink, "Dynamic electro thermal simulation of microsystems a review," *J. Micromech. Microeng.*, vol. 15, no. 11, pp. R17–R31, Nov. 2005.
- [2] V. d'Alessandro and N. Rinaldi, "A critical review of thermal models for electro-thermal simulation," *Solid State Electron.*, vol. 46, no. 4, pp. 487–496, Apr. 2002.
- [3] N. Rinaldi, "On the modeling of the transient thermal behavior of semiconductor devices," *IEEE Trans. Electron. Devices*, vol. 48, no. 12, pp. 2796–2802, Dec. 2001.
- [4] D. Celso, P. K. Gunupudi, R. Khazaka, D. J. Walkey, T. Smy, and M. S. Nakhla, "Fast simulation of steady-state temperature distributions in electronic components using multidimensional model reduction," *IEEE Trans. Compon. Packag. Technol.*, vol. 28, no. 1, pp. 70–79, Mar. 2005.
- [5] V. Camarchia, F. Cappelluti, M. Pirola, S. D. Guerrieri, and G. Ghione, "Self-consistent electrothermal modeling of class A, AB, and B power GaN HEMTs under modulated RF excitation," *IEEE Trans. Microw. Theory Tech.*, vol. 55, no. 9, pp. 1824–1831, Sep. 2007.
- [6] K. Poulton, K. L. Knudsen, and J. J. Corcoran, "Thermal design and simulation of bipolar integrated circuits," *IEEE J. Solid-State Circuits*, vol. 27, no. 10, pp. 1379–1387, Oct. 1992.
- [7] I. Marano, V. d'Alessandro, and N. Rinaldi, "Analytical modeling and numerical simulations of the thermal behavior of trench-isolated bipolar transistors," *Solid State Electron.*, vol. 53, no. 3, pp. 297–307, Mar. 2009.
- [8] W. Batty, A. Panks, R. Johnson, and C. Snowden, "Electrothermal modeling and measurement for spatial power combining at millimeter wavelengths," *IEEE Trans. Microw. Theory Tech.*, vol. 47, no. 12, pp. 2574–2585, Dec. 1999.
- [9] N. Jankovic, T. Pestic, and P. Igic, "All injection level power PIN diode model including temperature dependence," *Solid State Electron.*, vol. 51, no. 5, pp. 719–725, May 2007.
- [10] I. Melczarsky, J. A. Lonac, F. Filicori, and A. Santarelli, "Compact empirical modeling of nonlinear dynamic thermal effects in electron devices," *IEEE Trans. Microw. Theory Tech.*, vol. 56, no. 9, pp. 2017–2024, Sep. 2008.
- [11] W. Batty, C. E. Christoffersen, A. J. Panks, S. David, C. M. Snowden, and M. B. Steer, "Electrothermal CAD of power devices and circuits with fully physical temperature-dependent compact thermal modeling of complex nonlinear 3-D systems," *IEEE Trans. Compon. Packag. Technol.*, vol. 24, no. 4, pp. 566–590, Dec. 2001.
- [12] H. A. Mantooth and J. L. Duliere, "A unified diode model for circuit simulation," *IEEE Trans. Power Electron.*, vol. 12, no. 5, pp. 851–857, Sep. 1997.
- [13] K. Shinohara and Q. Yu, "Reliability evaluation of power semiconductor devices using coupled analysis simulation," in *Proc. 12th IEEE Intersoc. Conf. Thermal Thermomech. Phenom. Electron. Syst.*, Jun. 2–5, 2010, pp. 1–9.
- [14] M. Pokorny and Z. Raida, "Multi-physics model of Gunn diode," in *Proc. 17th Int. Conf. MIKON*, May 19–21, 2008, pp. 1–4.
- [15] A. Ammous, S. Ghedira, B. Allard, H. Morel, and D. Renault, "Choosing a thermal model for electrothermal simulation of power semiconductor devices," *IEEE Trans. Power Electron.*, vol. 14, no. 2, pp. 300–307, Mar. 1999.
- [16] V. Szekely, A. Poppe, A. Pahi, A. Csendes, G. Hajas, and M. Rencz, "Electrothermal and logi-thermal simulate on of VLSI designs," *IEEE Trans. Very Large Scale Integr. (VLSI) Syst.*, vol. 5, no. 3, pp. 258–269, Sep. 1997.
- [17] X. Chen, J. Q. Chen, K. Huang, and X. B. Xu, "A circuit simulation method based on physical approach for the analysis of Mot_bal99It1 p-i-n diode circuits," *IEEE Trans. Electron Devices*, vol. 58, no. 9, pp. 2862–2870, Sep. 2011.
- [18] A. Witzig, C. Schuster, P. Regli, and W. Fichtner, "Global modeling of microwave applications by combining the FDTD method and a general semiconductor device and circuit simulator," *IEEE Trans. Microw. Theory Tech.*, vol. 47, no. 6, pp. 919–928, Jun. 1999.
- [19] P. Ciampolini, L. Roselli, and G. Stopponi, "Integrated FDTD and solid-state device simulation," *IEEE Microw. Guid. Wave Lett.*, vol. 6, no. 11, pp. 419–421, Nov. 1996.
- [20] P. Ciampolini, L. Roselli, and G. Stopponi, "Mixed-mode circuit simulation with full-wave analysis of interconnections," *IEEE Trans. Electron Devices*, vol. 44, no. 11, pp. 2098–2105, Nov. 1997.
- [21] X. S. Xu, "A drift-diffusion model for semiconductors with temperature effects," in *Proc. Roy. Soc. Edinburgh Sec. A*, 2009, vol. 139, no. 5, pp. 1101–1119.
- [22] S. M. Sze, *Physics of Semiconductor Devices*. New York: Wiley, 1981.
- [23] M. Kurata, "Design considerations of step recovery diodes with the aid of numerical large-signal analysis," *IEEE Trans. Electron Devices*, vol. ED-19, no. 11, pp. 1207–1215, Nov. 1972.
- [24] C. Temperton, "Algorithms for the solution of cyclic tridiagonal systems," *J. Comput. Phys.*, vol. 19, no. 3, pp. 317–323, Nov. 1975.
- [25] R. Hefner and D. L. Blackburn, "Thermal component models for electrothermal network simulation," *IEEE Trans. Compon., Packag., Manuf. Technol.*, vol. 17, no. 3, pp. 413–424, Sep. 1994.
- [26] W. Sui, *Time-Domain Computer Analysis of Nonlinear Hybrid System*. Boca Raton, FL: CRC Press, 2002.



Jun-quan Chen is currently working toward the Ph.D. degree in radio physics in the College of Electronic and Information Engineering, Sichuan University, Sichuan, China.

His research interests include computational electromagnetics and antenna design.



Xing Chen (M'08–SM'09) received the Ph.D. degree in biomedical engineering from Sichuan University, Sichuan, China, in 2004.

He is currently a Professor with the College of Electronics and Information Engineering, Sichuan University.



Kama Huang (M'03–SM'04) received the Ph.D. degree from the University of Electronic Science and Technology, Chengdu, China, in 1991.

He has been with the College of Electronics and Information Engineering, Sichuan University, Chengdu, as Director since 1997.



Chang-Jun Liu (M'07–SM'09) received the Ph.D. degree from Sichuan University Chengdu, China, in 2000.

He is currently a Professor with the College of Electronics and Information Engineering, Sichuan University. His research interests include microwave components.



Xiao-Bang Xu (M'85–SM'91) received the Ph.D. degree in electrical engineering from the University of Mississippi, Oxford, in 1985.

He is currently a Full Professor in Holcombe Department of Electrical and Computer Engineering, Clemson University, Clemson, SC.